

Entanglement in Elastic and Inelastic Two-particle Scatterings at High Energy

Robi Peschanski*

*Institut de Physique Théorique[†], Université Paris-Saclay, CEA
F-91191 Gif-sur-Yvette, France*

and

Shigenori Seki[‡]

*Institute for Fundamental Sciences, Setsunan University
17-8 Ikeda-naka-machi, Neyagawa, Osaka 572-8508, Japan*

Abstract

We study the entanglement produced in transverse momentum by two-particle scattering at high energy. Employing the S-matrix framework for the derivation of reduced density matrices, we formulate the entanglement entropy for an inelastic scattering as well as an elastic one. We display the formulas of the entanglement entropy in terms of two-body cross sections. We also derive the entanglement density as a function of the transverse momentum. As an application, we then focus on both forward elastic ($pn \rightarrow pn$) and inelastic ($pn \rightarrow np$) channels scattering allowing for a fruitful comparison of the two reactions with the same proton-neutron content. We evaluate the elastic and inelastic entanglement entropy by using known parameterizations of experimental data for neutron-proton reactions. Comparing those entanglement entropies, we observe that the inelastic scattering produces more overall entanglement than the elastic one in the pn sector.

30 January 2026

*robi.peschanski@ipht.fr

[†]Unité Mixte de Recherche 3681 du CNRS

[‡]shigenori.seki@setsunan.ac.jp

1 Introduction

Quantum entanglement is one of the most significant phenomena in quantum physics, and many scientists in various fields have been studying it. In order to measure the strength of entanglement, one can use entanglement entropy. The density matrix, ρ , of a two-body state in a Hilbert space, $\mathcal{H}_A \otimes \mathcal{H}_B$, leads to the reduced density matrix, $\rho_A = \text{tr}_B \rho$. The entanglement entropy of that state is defined by $-\text{tr}_A \rho_A \ln \rho_A$. We are interested in the entanglement of two-body scattering. Even if the initial state of incoming particles are not entangled, the final state of outgoing particles should be entangled by interactions. So we ask a simple question, how much entanglement is produced by a two-body scattering process.

We consider the entanglement of the final state after scattering. In general, one can consider entanglements on various quantum numbers. For example, an entanglement of spin is one of the most well-known entanglements. We would like to reveal the entanglement on a momentum Hilbert space. The momentum-space entanglement in quantum field theory has been considered by Ref. [1]. In Ref. [2], the entanglement entropy of the final state in elastic scattering has been formulated by using an S-matrix theory. The formula of entanglement entropy in Ref. [2] is described in terms of physical quantities, *i.e.*, cross sections. However it includes a divergent factor yielded by the infinite volume of the momentum Hilbert space. In order to avoid this divergence, Ref. [3] has suggested the volume regularization, and has concretely evaluated such regularized entanglement entropy for proton-proton elastic scattering with parameterizations of the experimental data given by Tevatron in Fermilab and Large Hadron Collider in CERN. We can also see many other articles on the entanglement related to particle scattering, for instance, on scattering in QED [4–12], fermion-fermion scattering [13, 14], deep inelastic scattering [15–17], and so on [18–29].

In this paper, we consider the entanglement entropy of final states in inelastic scatterings as well as an elastic scattering. Although more than two particles can appear, and many more at high energies, as a final state in actual scattering processes, we concentrate on the entanglement of the two-particle final-state channels. We shall formulate the entanglement entropy of the two-particle final state for inelastic scatterings by using the S-matrix theory, as Refs. [2, 3] have done for an elastic scattering, keeping both derivations in parallel.

We shall concretely evaluate the entanglement entropy in elastic and inelastic channels. Although we can consider many examples of scattering, we focus on a proton-neutron scattering, which allows for elastic or inelastic channels, depending on considering the forward region in $pn \rightarrow pn$ or $pn \rightarrow np$ scattering. There are thus two channels; $pn \rightarrow pn$ and

$pn \rightarrow np$, with same initial and final particle content. We call the former the elastic channel and the latter the inelastic one. We distinguish them in our formulation from the viewpoint of the exchange of t -channel quantum numbers. We can practically find the appropriate parameterizations of experimental data for both channels from various reactions of neutron projectiles on fixed target experiments at high energy.

As an interesting by-product of our analysis, we obtain the density distribution of the entanglement entropy as a function of transverse momentum, allowing for obtaining a hint of the entanglement flow during the scattering process in both elastic and inelastic cases.

In Section 2, we review the S-matrix formalism with partial wave expansions [30, 31]. In Section 3, using this formalism, we define the density matrices and formulate the entanglement entropy for two-particle final states both in elastic and inelastic channels. We then obtain the distribution density of the entanglement entropy as a function of momentum transfer. In Section 4, we evaluate the entanglement entropy and its transverse momentum distribution for proton-neutron scattering from known parameterizations of the experimental data, and clarify the difference of entanglement entropy between the elastic and inelastic channels. Section 5 is dedicated to discussion, conclusions and outlook.

2 Entanglement entropy in the S-matrix formulation

Since we are interested in the entanglement entropy of general two-particle states at high energy, we are led to consider three kinds of scattering channels as follows:

$$A_1 B_1 \rightarrow \begin{cases} A_1 B_1 & \text{(elastic channel)} \\ A_n B_n \quad (i = 2, 3, \dots) & \text{(two-particle inelastic channels)} \\ X & \text{(more than two-particle channels)} \end{cases} \quad (2.1)$$

The initial state consists of two particles, A_1 and B_1 , and the final states are $A_1 B_1$, $A_n B_n$ ($n = 2, 3, \dots$) and the multi-particle states, X . In the two-particle inelastic channels, the pair of A_1 and B_1 is different from the one of A_2 and B_2 , but it is not necessary that both A_1 and B_1 are different from A_n and B_n , namely, for example, combinations of $A_n = A_1$ and $B_n \neq B_1$ are allowed. Furthermore, $A_1 B_1$ may be different from $B_1 A_1$ in our formulation and classified into the inelastic channels, if corresponding to a scattering with non-vacuum quantum number exchange.

We shall formulate the entanglement entropy of two-particle states in terms of the S-matrix formalism. For sake of simplicity we will stick to the formalism with only one inelastic

channel, *i.e.*,

$$A_1B_1 \rightarrow \begin{cases} A_1B_1 & \text{(elastic channel)} \\ A_2B_2 & \text{(two-particle inelastic channel)} \\ X & \text{(more than two-particle channels)} \end{cases} \quad (2.2)$$

at high energy [30] but the generalization of the formalism to a finite set of two-body inelastic channels has also been done in matrix form [31], which can be easily applied.

2.1 S-matrix and unitarity

Following Ref. [30], we shall adjust the S-matrix theory for the scattering including a two-particle inelastic channel together with the elastic one.

The Hilbert spaces of two particle states, A_1B_1 and A_2B_2 , are respectively

$$\mathcal{H}_1 = \mathcal{H}_{A_1} \otimes \mathcal{H}_{B_1}, \quad \mathcal{H}_2 = \mathcal{H}_{A_2} \otimes \mathcal{H}_{B_2}. \quad (2.3)$$

Each Hilbert space \mathcal{H}_I ($I = A_1, B_1, A_2, B_2$) is the Fock space of the particle I . The state of I with momentum \mathbf{p} in \mathcal{H}_I is denoted by $|\mathbf{p}\rangle_I \in \mathcal{H}_I$. The inner products of the states is defined as

$${}_I\langle \mathbf{p} | \mathbf{q} \rangle_J = \delta_{IJ} \sqrt{2E_{I\mathbf{p}} 2E_{J\mathbf{q}}} \delta^{(3)}(\mathbf{p} - \mathbf{q}), \quad (2.4)$$

where the energy $E_{I\mathbf{p}} = \sqrt{m_I^2 + \mathbf{p}^2}$ ($p \equiv |\mathbf{p}|$). The total Hilbert space concerning the scattering process (2.2) is given by $\mathcal{H}_{\text{tot}} = \mathcal{H}_1 \otimes \mathcal{H}_2 \otimes \mathcal{H}_X$, where \mathcal{H}_X is the Hilbert space for multi-particle states, *i.e.* for more than two particles in the final state. We describe states in \mathcal{H}_1 and \mathcal{H}_2 as

$$|\mathbf{p}, \mathbf{q}\rangle_1 \equiv |\mathbf{p}\rangle_{A_1} \otimes |\mathbf{q}\rangle_{B_1} \in \mathcal{H}_1, \quad |\mathbf{p}, \mathbf{q}\rangle_2 \equiv |\mathbf{p}\rangle_{A_2} \otimes |\mathbf{q}\rangle_{B_2} \in \mathcal{H}_2, \quad (2.5)$$

for the sake of convenience. The complete set given by orthogonal basis satisfies

$$\mathbf{1} = \int \frac{d^3\mathbf{p} d^3\mathbf{q}}{2E_{A_1\mathbf{p}} 2E_{B_1\mathbf{q}}} |\mathbf{p}, \mathbf{q}\rangle_1 \langle \mathbf{p}, \mathbf{q}| + \int \frac{d^3\mathbf{p} d^3\mathbf{q}}{2E_{A_2\mathbf{p}} 2E_{B_2\mathbf{q}}} |\mathbf{p}, \mathbf{q}\rangle_2 \langle \mathbf{p}, \mathbf{q}| + \int dX |X\rangle \langle X|, \quad (2.6)$$

where $\mathbf{1}$ is the unit matrix.

We introduce the well-known S-matrix, \mathcal{S} , relating the set of asymptotic final states to the initial pair of states. The transition T-matrix, \mathcal{T} , which describes the scattering amplitudes is such that $\mathcal{S} = \mathbf{1} + 2i\mathcal{T}$. The unitarity of the S-matrix corresponding to the completeness of the final state basis writes $\mathcal{S}^\dagger \mathcal{S} = \mathbf{1}$. It is equivalently expressed in terms of the T-matrix,

$$\frac{1}{2i} (\mathcal{T} - \mathcal{T}^\dagger) = \mathcal{T}^\dagger \mathcal{T}. \quad (2.7)$$

In terms of Eq. (2.6), the unitarity condition (2.7) leads to a relation of the T-matrix elements concerning the two-particle states, ${}_i\langle \mathbf{p}, \mathbf{q} |$ and $|\mathbf{p}', \mathbf{q}'\rangle_j$;

$$\begin{aligned} & \frac{1}{2i} \{ {}_i\langle \mathbf{p}, \mathbf{q} | \mathcal{T} | \mathbf{p}', \mathbf{q}'\rangle_j - {}_i\langle \mathbf{p}, \mathbf{q} | \mathcal{T}^\dagger | \mathbf{p}', \mathbf{q}'\rangle_j \} \\ &= \sum_{h=1}^2 \int \frac{d^3 \mathbf{p}''}{2E_{A_h} \mathbf{p}''} \frac{d^3 \mathbf{q}''}{2E_{B_h} \mathbf{q}''} {}_i\langle \mathbf{p}, \mathbf{q} | \mathcal{T}^\dagger | \mathbf{p}'', \mathbf{q}''\rangle_h {}_h\langle \mathbf{p}'', \mathbf{q}'' | \mathcal{T} | \mathbf{p}', \mathbf{q}'\rangle_j \\ &+ \int dX {}_i\langle \mathbf{p}, \mathbf{q} | \mathcal{T}^\dagger | X \rangle \langle X | \mathcal{T} | \mathbf{p}', \mathbf{q}'\rangle_j \quad (i, j = 1, 2). \end{aligned} \quad (2.8)$$

2.2 Overlap matrix and partial wave expansion

Let us adopt the center-of-mass frame. We describe the states (2.5) as

$$|\mathbf{p}\rangle\!\rangle_1 \equiv |\mathbf{p}, -\mathbf{p}\rangle_1, \quad |\mathbf{p}\rangle\!\rangle_2 \equiv |\mathbf{p}, -\mathbf{p}\rangle_2, \quad (2.9)$$

and the inner product of states becomes

$${}_i\langle\langle \mathbf{p} | \mathbf{q} \rangle\rangle_j = \delta_{ij} 2E_{A_i} \mathbf{p} 2E_{B_i} \mathbf{p} \delta^{(3)}(\mathbf{p} - \mathbf{q}) \delta^{(3)}(0) \quad (i, j = 1, 2). \quad (2.10)$$

In terms of these expressions, the complete set of orthogonal basis (2.6) is rewritten as

$$\mathbf{1} = \sum_{h=1}^2 \int \frac{d^3 \mathbf{p}}{2E_{A_h} \mathbf{p} 2E_{B_h} \mathbf{p} \delta^{(3)}(0)} |\mathbf{p}\rangle\!\rangle_h {}_h\langle\langle \mathbf{p}| + \int dX |X\rangle \langle X|. \quad (2.11)$$

We extract the factors of energy-momentum conservation from the T-matrix elements,

$${}_i\langle\langle \mathbf{p} | \mathcal{T} | \mathbf{q} \rangle\rangle_j = {}_i\langle\langle \mathbf{p} | \mathbf{t} | \mathbf{q} \rangle\rangle_j \delta^{(4)}(\mathcal{P}_{i\mathbf{p}} - \mathcal{P}_{j\mathbf{q}}), \quad {}_i\langle\langle \mathbf{p} | \mathcal{T} | X \rangle\rangle = {}_i\langle\langle \mathbf{p} | \mathbf{t} | X \rangle\rangle \delta^{(4)}(\mathcal{P}_{i\mathbf{p}} - \mathcal{P}_X), \quad (2.12)$$

where $\mathcal{P}_{i\mathbf{p}}$ and \mathcal{P}_X are the total energy-momenta of the states $|\mathbf{p}\rangle\!\rangle_i$ and $|X\rangle$ respectively. For example, the first delta function in (2.12) stands for

$$\begin{aligned} \delta^{(4)}(\mathcal{P}_{i\mathbf{p}} - \mathcal{P}_{j\mathbf{q}}) &= \delta^{(3)}((\mathbf{p} + (-\mathbf{p})) - (\mathbf{q} + (-\mathbf{q}))) \delta((E_{A_i} \mathbf{p} + E_{B_i} \mathbf{p}) - (E_{A_j} \mathbf{q} + E_{B_j} \mathbf{q})) \\ &= \delta^{(3)}(0) \delta((E_{A_i} \mathbf{p} + E_{B_i} \mathbf{p}) - (E_{A_j} \mathbf{q} + E_{B_j} \mathbf{q})). \end{aligned} \quad (2.13)$$

Since some factors of energy-momentum conservation in Eq. (2.8) are cancelled in the center-of-mass frame, one can rewrite the condition (2.8) as

$$\begin{aligned} & \frac{1}{2i} ({}_i\langle\langle \mathbf{q} | \mathbf{t} | \mathbf{k} \rangle\rangle_j - {}_i\langle\langle \mathbf{q} | \mathbf{t}^\dagger | \mathbf{k} \rangle\rangle_j) \\ &= \sum_{h=1}^2 \int \frac{d^3 \mathbf{q}}{2E_{A_h} \mathbf{q} 2E_{B_h} \mathbf{q} \delta^{(3)}(0)} {}_i\langle\langle \mathbf{q} | \mathbf{t}^\dagger | \mathbf{q} \rangle\rangle_h \delta^{(4)}(\mathcal{P}_{h\mathbf{q}} - \mathcal{P}_{j\mathbf{k}}) {}_h\langle\langle \mathbf{q} | \mathbf{t} | \mathbf{k} \rangle\rangle_j + F_{ij}(\mathbf{p}, \mathbf{k}), \end{aligned} \quad (2.14)$$

where $F_{ij}(\mathbf{p}, \mathbf{k})$ is an overlap matrix [30],

$$F_{ij}(\mathbf{p}, \mathbf{k}) = \int dX \langle\langle \mathbf{p} | \mathbf{t}^\dagger | X \rangle\rangle \delta^{(4)}(P_X - P_{j\mathbf{k}}) \langle X | \mathbf{t} | \mathbf{k} \rangle\rangle_j. \quad (2.15)$$

The delta functions for energy conservation in Eq. (2.14) imply that the center-of-mass energies of the states are common, that is,

$$E_{A_i\mathbf{p}} + E_{B_i\mathbf{p}} = E_{A_j\mathbf{k}} + E_{B_j\mathbf{k}} = E_{A_h\mathbf{q}} + E_{B_h\mathbf{q}} \equiv \sqrt{s}. \quad (2.16)$$

s is the usual Mandelstam variable.

We expand a T-matrix element and the overlap matrix in partial waves,

$$\langle\langle \mathbf{p} | \mathbf{t} | \mathbf{k} \rangle\rangle_j = \frac{\sqrt{s}}{\pi \sqrt{pk}} \sum_{\ell=1}^{\infty} (2\ell + 1) \tau_{ij}^\ell P_\ell(\cos \theta), \quad (2.17)$$

$$F_{ij}(\mathbf{p}, \mathbf{k}) = \frac{\sqrt{s}}{2\pi \sqrt{pk}} \sum_{\ell=1}^{\infty} (2\ell + 1) f_{ij}^\ell P_\ell(\cos \theta), \quad (2.18)$$

where the scattering angle, θ , is defined by $\mathbf{p} \cdot \mathbf{k} = pk \cos \theta$. Then, by using partial wave modes in Eqs. (2.17) and (2.18), one can express the unitarity condition (2.14) in the following simple form;

$$\text{Im } \tau_{ij}^\ell = \sum_{h=1}^2 \tau_{ih}^{\ell*} \tau_{hj}^\ell + \frac{1}{2} f_{ij}^\ell. \quad (2.19)$$

2.3 Cross sections

The two-body scattering amplitude $\mathcal{A}_{ij}(s, t)$ is of the channel: $A_j B_j \rightarrow A_i B_i$ with the initial state, $|\mathbf{k}\rangle\rangle_j$, and the final state, $|\mathbf{p}\rangle\rangle_i$. It is related with the S-matrix element, $\langle\langle \mathbf{p} | \mathbf{s} | \mathbf{k} \rangle\rangle_j$, as follows:

$$\langle\langle \mathbf{p} | \mathbf{s} | \mathbf{k} \rangle\rangle_j = \frac{\sqrt{s}}{\pi \sqrt{pk}} \cdot 2 \left(\delta(1 - \cos \theta) \delta_{ij} + \frac{i}{16\pi} \mathcal{A}_{ij}(s, t) \right). \quad (2.20)$$

\mathbf{s} is defined by $\mathbf{s} = \mathbf{1} + 2i\mathbf{t}$, while s and t are the Mandelstam variables, here given by

$$\sqrt{s} = \sqrt{m_{A_j}^2 + k^2} + \sqrt{m_{B_j}^2 + k^2}, \quad t = 2k^2(\cos \theta - 1). \quad (2.21)$$

Thus \mathcal{A}_{ij} is described in terms of the partial wave modes as

$$\mathcal{A}_{ij} = 16\pi \sum_{\ell=0}^{\infty} (2\ell + 1) \tau_{ij}^\ell P_\ell(\cos \theta). \quad (2.22)$$

Since the differential cross section is

$$\frac{d\sigma_{ij}}{dt} = \frac{\pi}{k^4} \left| \sum_{\ell=0}^{\infty} (2\ell+1) \tau_{ij}^{\ell} P_{\ell}(\cos \theta) \right|^2 = \frac{|\mathcal{A}_{ij}|^2}{256\pi k^4}, \quad (2.23)$$

we obtain the cross section of the two-particle final states, thanks to the orthogonality property of Legendre polynomials,

$$\sigma_{ij} = \frac{4\pi}{k^2} \sum_{\ell=0}^{\infty} (2\ell+1) |\tau_{ij}^{\ell}|^2. \quad (2.24)$$

If $i = j$, σ_{ii} is the elastic cross section, while if $i \neq j$, σ_{ij} is the two-particle inelastic cross section. One can also obtain the cross section for multi-particle inelastic channel from the overlap matrix modes, namely

$$\sigma_{ij}^X = \frac{2\pi}{k^2} \sum_{\ell=0}^{\infty} (2\ell+1) f_{ij}^{\ell}. \quad (2.25)$$

When we set the initial state to be $A_1 B_1$, the unitarity condition (2.19) implies

$$\text{Im } \tau_{11}^{\ell} = |\tau_{11}^{\ell}|^2 + |\tau_{21}^{\ell}|^2 + \frac{1}{2} f_{11}^{\ell}. \quad (2.26)$$

Then the total cross section is given by

$$\sigma_{11}^{\text{tot}} = \frac{4\pi}{k^2} \sum_{\ell=0}^{\infty} (2\ell+1) \text{Im } \tau_{11}^{\ell} = \sigma_{11} + \sigma_{21} + \sigma_{11}^X. \quad (2.27)$$

3 Formulation of entanglement entropy

3.1 Density matrices of two-body elastic and inelastic final states

We consider the scattering processes (2.2). The two particles, $A_1 B_1$, in the initial state $|\text{ini}\rangle$ have momenta, \mathbf{k} and \mathbf{l} , respectively, *i.e.*, $|\text{ini}\rangle = |\mathbf{k}, \mathbf{l}\rangle_1$. Then, in terms of the S-matrix, the final state is given by $\mathcal{S}|\text{ini}\rangle \in \mathcal{H}_{\text{tot}}$. By using the projection from \mathcal{H}_{tot} to \mathcal{H}_1 , we obtain the final state as $A_1 B_1$ in the elastic channel,

$$|\text{fin}\rangle_1 = \left(\int \frac{d^3\mathbf{p}}{2E_{A_1\mathbf{p}}} \frac{d^3\mathbf{q}}{2E_{B_1\mathbf{q}}} |\mathbf{p}, \mathbf{q}\rangle_1 \langle \mathbf{p}, \mathbf{q}| \right) \mathcal{S} |\mathbf{k}, \mathbf{l}\rangle_1 = \int \frac{d^3\mathbf{p}}{2E_{A_1\mathbf{p}}} \frac{d^3\mathbf{q}}{2E_{B_1\mathbf{q}}} |\mathbf{p}, \mathbf{q}\rangle_1 \langle \mathbf{p}, \mathbf{q}| (1 + 2i\mathcal{T}) |\mathbf{k}, \mathbf{l}\rangle_1. \quad (3.1)$$

In the same way, the final state as $A_2 B_2$ in the two-particle inelastic channel is

$$|\text{fin}\rangle_2 = \left(\int \frac{d^3\mathbf{p}}{2E_{A_2\mathbf{p}}} \frac{d^3\mathbf{q}}{2E_{B_2\mathbf{q}}} |\mathbf{p}, \mathbf{q}\rangle_2 \langle \mathbf{p}, \mathbf{q}| \right) \mathcal{S} |\mathbf{k}, \mathbf{l}\rangle_1 = \int \frac{d^3\mathbf{p}}{2E_{A_2\mathbf{p}}} \frac{d^3\mathbf{q}}{2E_{B_2\mathbf{q}}} |\mathbf{p}, \mathbf{q}\rangle_2 \langle \mathbf{p}, \mathbf{q}| 2i\mathcal{T} |\mathbf{k}, \mathbf{l}\rangle_1. \quad (3.2)$$

Note the essential difference between Eqs. (3.1) and (3.2): The unit matrix in \mathcal{S} does not contribute to the final state in the inelastic channel due to ${}_2\langle \mathbf{p}, \mathbf{q} | \mathbf{1} | \mathbf{k}, \mathbf{l} \rangle_1 = 0$.

By using these final states, we define the total density matrices of final two-body states as

$$\rho_1 = \frac{1}{\mathcal{N}_1} |\text{fin}\rangle_1 {}_1\langle \text{fin}|, \quad \rho_2 = \frac{1}{\mathcal{N}_2} |\text{fin}\rangle_2 {}_2\langle \text{fin}|. \quad (3.3)$$

\mathcal{N}_i ($i = 1, 2$) are normalization factors which are determined by $\text{tr}_{A_i} \text{tr}_{B_i} \rho_i = 1$.

We then obtain reduced density matrices from the total density matrices by taking trace on one of the Hilbert spaces of two particles. In the case of elastic channel, we calculate the reduced density matrix, $\rho_{A_1} = \text{tr}_{B_1} \rho_1$, with extracting the factor of energy-momentum conservation from the expression (3.1),

$$\begin{aligned} \rho_{A_1} &= \int \frac{d^3 \mathbf{r}}{2E_{B_1} \mathbf{r}} {}_{B_1}\langle \mathbf{r} | \rho_1 | \mathbf{r} \rangle_{B_1} \\ &= \frac{1}{\mathcal{N}_1} \int \frac{d^3 \mathbf{p}}{2E_{A_1} \mathbf{p}} \frac{\delta(E_{A_1} \mathbf{p} + E_{B_1(\mathbf{k}+\mathbf{l}-\mathbf{p})} - E_{A_1} \mathbf{k} - E_{B_1} \mathbf{l}) \delta(0)}{2E_{A_1} \mathbf{p} 2E_{B_1(\mathbf{k}+\mathbf{l}-\mathbf{p})}} | {}_1\langle \mathbf{p}, \mathbf{k} + \mathbf{l} - \mathbf{p} | \mathbf{s} | \mathbf{k}, \mathbf{l} \rangle_1 |^2 | \mathbf{p} \rangle_{A_1} {}_{A_1}\langle \mathbf{p} |. \end{aligned} \quad (3.4)$$

Although there is a divergent factor, $\delta(0)$, we leave it for the present and shall regularize it later. In the same way, the reduced density matrix, $\rho_{A_2} = \text{tr}_{B_2} \rho_2$, for the case of two-particle inelastic channel is described as

$$\begin{aligned} \rho_{A_2} &= \int \frac{d^3 \mathbf{r}}{2E_{B_2} \mathbf{r}} {}_{B_2}\langle \mathbf{r} | \rho_2 | \mathbf{r} \rangle_{B_2} \\ &= \frac{1}{\mathcal{N}_2} \int \frac{d^3 \mathbf{p}}{2E_{A_2} \mathbf{p}} \frac{\delta(E_{A_2} \mathbf{p} + E_{B_2(\mathbf{k}+\mathbf{l}-\mathbf{p})} - E_{A_2} \mathbf{k} - E_{B_2} \mathbf{l}) \delta(0)}{2E_{A_2} \mathbf{p} 2E_{B_2(\mathbf{k}+\mathbf{l}-\mathbf{p})}} | {}_2\langle \mathbf{p}, \mathbf{k} + \mathbf{l} - \mathbf{p} | 4\mathbf{t} | \mathbf{k}, \mathbf{l} \rangle_1 |^2 | \mathbf{p} \rangle_{A_2} {}_{A_2}\langle \mathbf{p} |. \end{aligned} \quad (3.5)$$

Note again the difference between the matrix elements in Eqs. (3.4) and (3.5).

3.2 Entanglement entropy

In this subsection, we adopt the center-of-mass frame again. The momenta of the initial state satisfy $\mathbf{l} = -\mathbf{k}$, and the center-of-mass energy is $\sqrt{s} = E_{A_1} \mathbf{k} + E_{B_1} \mathbf{k}$.

We firstly calculate $\text{tr}_{A_i}(\rho_{A_i})^n$, which is related to the Rényi entropy, $(1-n)^{-1} \ln \text{tr}_{A_i}(\rho_{A_i})^n$. Then it gives us the entanglement entropy through

$$S_{i1} = -\text{tr}_{A_i} \rho_{A_i} \ln \rho_{A_i} = -\lim_{n \rightarrow 1} \frac{\partial}{\partial n} \text{tr}_{A_i}(\rho_{A_i})^n. \quad (3.6)$$

S_{i1} denotes the entanglement entropy of the final state in the channel: $A_1 B_1 \rightarrow A_i B_i$. This observable serves as a measure of the entanglement between the two particles in each final state.

3.2.1 Elastic channel

Since the entanglement entropy between two particles in the elastic scattering has been formulated by Ref. [2], we here calculate the elastic entanglement entropy in our current notation allowing for a parallel calculation between the elastic and inelastic cases.

In the center-of-mass frame, the reduced density matrix (3.4) becomes

$$\rho_{A_1} = \frac{1}{\mathcal{N}_1} \int \frac{d^3 \mathbf{p}}{2E_{A_1 \mathbf{p}}} \frac{\delta(p - k)\delta(0)}{4p\sqrt{s}} |_1 \langle \langle \mathbf{p} | \mathbf{s} | \mathbf{k} \rangle \rangle_1|^2 | \mathbf{p} \rangle_{A_1} \langle \mathbf{p} | , \quad (3.7)$$

where we used

$$\delta(E_{A_1 \mathbf{p}} + E_{B_1 \mathbf{p}} - \sqrt{s}) = \frac{2E_{A_1 \mathbf{p}} 2E_{B_1 \mathbf{p}}}{4p\sqrt{s}} \delta(p - k) . \quad (3.8)$$

The normalization factor \mathcal{N}_1 is determined by $1 = \text{tr}_{A_1} \text{tr}_{B_1} \rho_1 = \text{tr}_{A_1} \rho_{A_1}$, so that

$$\mathcal{N}_1 = \delta(0)\delta^{(3)}(0) \int d^3 \mathbf{p} \frac{\delta(p - k)}{4p\sqrt{s}} |_1 \langle \langle \mathbf{p} | \mathbf{s} | \mathbf{k} \rangle \rangle_1|^2 . \quad (3.9)$$

Then we calculate

$$\text{tr}_{A_1}(\rho_{A_1})^n = \int d^3 \mathbf{p} \delta^{(3)}(0) \left(\frac{\delta(p - k)\delta(0)}{\mathcal{N}_1 \cdot 4p\sqrt{s}} |_1 \langle \langle \mathbf{p} | \mathbf{s} | \mathbf{k} \rangle \rangle_1|^2 \right)^n . \quad (3.10)$$

Now we use the partial wave expansion (2.17) and (2.18). The normalization factor (3.9) is written as

$$\mathcal{N}_1 = \delta(0)\delta^{(3)}(0) \frac{\sqrt{s}}{\pi k} \sum_{\ell=0}^{\infty} (2\ell + 1) |s_{11}^{\ell}|^2 , \quad (3.11)$$

where the partial wave mode s_{ij}^{ℓ} is defined as $s_{ij}^{\ell} = \delta_{ij} + 2i\tau_{ij}^{\ell}$. Then Eq. (3.10) becomes

$$\text{tr}_{A_1}(\rho_{A_1})^n = \int_{-1}^1 d\cos \theta \left(\frac{\delta(0)}{2\pi k^2 \delta^{(3)}(0)} \right)^{n-1} (\mathcal{P}_{11}(\cos \theta))^n , \quad (3.12)$$

$$\mathcal{P}_{11}(\cos \theta) \equiv \frac{|\sum_{\ell=0}^{\infty} (2\ell + 1) s_{11}^{\ell} P_{\ell}(\cos \theta)|^2}{2 \sum_{\ell=0}^{\infty} (2\ell + 1) |s_{11}^{\ell}|^2} , \quad (3.13)$$

after the integration over the spherical coordinates of \mathbf{p} with azimuthal symmetry.

The “volume” V of momentum Hilbert space is infinite. Indeed it can be formally written as

$$V \equiv \sum_{\ell=0}^{\infty} (2\ell + 1) = 2\delta(0). \quad (3.14)$$

Note that with this definition, V is dimensionless. The delta function appears due to the property of Legendre polynomials, $2\delta(1 - x) = \sum_{\ell=0}^{\infty} (2\ell + 1)P_{\ell}(x)$, with $P_{\ell}(0) = 1$. The factor in the right hand side of Eq. (3.12), $\delta(0)/(2\pi k^2 \delta^{(3)}(0))$, is equal to $2/V$ (see Eq. (A.2)). Therefore Eq. (3.12) may be rewritten as

$$\text{tr}_{A_1}(\rho_{A_1})^n = \left(\frac{2}{V}\right)^{n-1} \int_{-1}^1 d\cos\theta (\mathcal{P}_{11}(\cos\theta))^n. \quad (3.15)$$

By using the cross sections (2.23), (2.24) and (2.27), we can rewrite Eq. (3.13) as

$$\mathcal{P}_{11}(\cos\theta) = \delta(1 - \cos\theta) \left\{ 1 - \frac{\sigma_{11}}{\frac{\pi}{k^2}V - (\sigma_{11}^{\text{tot}} - \sigma_{11})} \right\} + \frac{2k^2}{\frac{\pi}{k^2}V - (\sigma_{11}^{\text{tot}} - \sigma_{11})} \frac{d\sigma_{11}}{dt}. \quad (3.16)$$

Note that $\sigma_{11}^{\text{tot}} - \sigma_{11}$ is equal to the sum of all inelastic cross sections, $\sigma_{21} + \sigma_{11}^X$. \mathcal{P}_{11} depends on the infinite volume of Hilbert space, V . Refs. [2, 3] have suggested to regularize it by “volume regularization”, see the next subsection.

Finally, we obtain the entanglement entropy of the elastic channel,

$$S_{11} = -\lim_{n \rightarrow 1} \frac{\partial}{\partial n} \text{tr}_{A_1}(\rho_{A_1})^n = \ln \frac{V}{2} - \int_{-1}^1 d\cos\theta \mathcal{P}_{11}(\cos\theta) \ln \mathcal{P}_{11}(\cos\theta), \quad (3.17)$$

where we used $\int_{-1}^1 d\cos\theta \mathcal{P}_{11}(\cos\theta) = 1$.

3.2.2 Inelastic two-particle channel

In the center-of-mass frame, the reduced density matrix (3.5) becomes

$$\rho_{A_2} = \frac{1}{\mathcal{N}_2} \int \frac{d^3\mathbf{p}}{2E_{A_2}\mathbf{p}} \frac{\delta(p - k')\delta(0)}{p\sqrt{s}} |_2\langle\langle \mathbf{p}|\mathbf{t}|\mathbf{k}\rangle\rangle_1|^2 |\mathbf{p}\rangle_{A_2} \langle \mathbf{p}|, \quad (3.18)$$

where

$$k' = \sqrt{\frac{(m_{A_2}^2 + m_{B_2}^2 - s)^2 - 4m_{A_2}^2 m_{B_2}^2}{4s}}. \quad (3.19)$$

The details of this calculation are shown in Appendix B. Note that k' satisfies $E_{A_2 k'} + E_{B_2 k'} = \sqrt{s}$. The normalization factor \mathcal{N}_2 is determined by $1 = \text{tr}_{A_2} \text{tr}_{B_2} \rho_2 = \text{tr}_{A_2} \rho_{A_2}$, so that

$$\mathcal{N}_2 = \delta(0)\delta^{(3)}(0) \int d^3\mathbf{p} \frac{\delta(p - k')}{p\sqrt{s}} |_2\langle\langle \mathbf{p}|\mathbf{t}|\mathbf{k}\rangle\rangle_1|^2. \quad (3.20)$$

From Eq. (3.18), we calculate

$$\mathrm{tr}_{A_2}(\rho_{A_2})^n = \int d^3\mathbf{p} \delta^{(3)}(0) \left(\frac{\delta(p - k')\delta(0)}{\mathcal{N}_2 \cdot p\sqrt{s}} |_2 \langle \langle \mathbf{p} | \mathbf{t} | \mathbf{k} \rangle \rangle_1|^2 \right)^n. \quad (3.21)$$

Substituting the partial wave expansions (2.17) and (2.18) into Eqs. (3.20) and (3.21), we obtain

$$\mathrm{tr}_{A_2}(\rho_{A_2})^n = \int d\cos\theta \left(\frac{\delta(0)}{2\pi k'^2 \delta^{(3)}(0)} \right)^{n-1} (\mathcal{P}_{21}(\cos\theta))^n, \quad (3.22)$$

$$\mathcal{P}_{21}(\cos\theta) \equiv \frac{|\sum_{\ell=0}^{\infty} (2\ell+1) \tau_{21}^{\ell} P_{\ell}(\cos\theta)|^2}{2 \sum_{\ell=0}^{\infty} (2\ell+1) |\tau_{21}^{\ell}|^2}. \quad (3.23)$$

By using the cross sections (2.23) and (2.24), Eq. (3.23) is described as

$$\mathcal{P}_{21}(\cos\theta) = \frac{2k^2}{\sigma_{21}} \frac{d\sigma_{21}}{dt}. \quad (3.24)$$

\mathcal{P}_{21} satisfies $\int_{-1}^1 d\cos\theta \mathcal{P}_{21}(\cos\theta) = 1$ in the same way as \mathcal{P}_{11} . Eq. (3.24) has simpler expression than Eq. (3.16), because the unit matrix part of S-matrix, $\mathbf{1}$, in $\mathbf{s} = \mathbf{1} + 2i\mathbf{t}$ does not contribute to \mathcal{P}_{21} in the inelastic channel, but it does to \mathcal{P}_{11} in the elastic channel. Therefore \mathcal{P}_{21} is finite and does not depend on the infinite volume of Hilbert space, V .

In terms of Eq. (A.2), Eq. (3.22) becomes

$$\mathrm{tr}_{A_2}(\rho_{A_2})^n = \left(\frac{2}{V} \right)^{n-1} \int_{-1}^1 d\cos\theta (\mathcal{P}_{21}(\cos\theta))^n. \quad (3.25)$$

We thus obtain the entanglement entropy,

$$S_{21} = - \lim_{n \rightarrow 1} \frac{\partial}{\partial n} \mathrm{tr}_{A_2}(\rho_{A_2})^n = \ln \frac{V}{2} - \int_{-1}^1 d\cos\theta \mathcal{P}_{12}(\cos\theta) \ln \mathcal{P}_{21}(\cos\theta) \quad (3.26)$$

By using the Mandelstam variable t , we can also rewrite S_{21} as

$$S_{21} = \ln \frac{V}{2} - \int_{-4k^2}^0 dt \frac{1}{\sigma_{21}} \frac{d\sigma_{21}}{dt} \ln \left(\frac{2k^2}{\sigma_{21}} \frac{d\sigma_{21}}{dt} \right). \quad (3.27)$$

We note that S_{11} for the elastic two-particle final state and S_{21} for the inelastic two-particle final state have a common diverging factor, $\ln(V/2)$.

3.3 Regularization of infinite Hilbert space volume

Let us regularize the infinite volume V in the same way as Ref. [3], which is the volume regularization. In Eq. (3.16), the first term is the contribution of non-interacting process,

because it is non-zero only if the scattering angle θ is equal to zero. Therefore, in order to erase this term, which would be interpreted as the contribution of non-interacting initial states, we set the “regularized volume” \tilde{V} , again dimensionless, to be determined by the cancelation of the coefficient of the δ -function in Eq. (3.16), namely

$$\tilde{V} \equiv \frac{k^2}{\pi} \sigma_{11}^{\text{tot}}. \quad (3.28)$$

It is important to note that \tilde{V} depends only on the total cross-section of the incoming particles. Hence, in particular, \tilde{V} is identical for elastic and inelastic two-body scattering from the same initial particles.

Then the entanglement entropy for elastic channel (3.17) is regularized,

$$\tilde{S}_{11} = \ln \frac{k^2 \sigma_{11}^{\text{tot}}}{2\pi} - \int_{-1}^1 d\cos \theta \tilde{\mathcal{P}}_{11} \ln \tilde{\mathcal{P}}_{11}, \quad \tilde{\mathcal{P}}_{11} = \frac{1}{\sigma_{11}} \frac{d\sigma_{11}}{d\cos \theta}, \quad (3.29)$$

while the entanglement entropy for inelastic channel (3.27) is

$$\tilde{S}_{21} = \ln \frac{k^2 \sigma_{11}^{\text{tot}}}{2\pi} - \int_{-1}^1 d\cos \theta \mathcal{P}_{21} \ln \mathcal{P}_{21}, \quad \mathcal{P}_{21} = \frac{1}{\sigma_{21}} \frac{d\sigma_{21}}{d\cos \theta}. \quad (3.30)$$

Note that $\tilde{\mathcal{P}}_{11}$ is regularized, while \mathcal{P}_{21} has not to be. However, it is interesting that $\tilde{\mathcal{P}}_{11}$ and \mathcal{P}_{21} finally have identical forms in terms of normalized two-body cross sections.

We can easily generalize these results to the case of the scattering including more channels of two-particle final states, (2.1). The entanglement entropy of the final state, $A_i B_i$ ($i = 2, 3, \dots$), without regularization is

$$S_{i1} = \ln \frac{V}{2} - \int_{-1}^1 d\cos \theta \mathcal{P}_{i1} \ln \mathcal{P}_{i1}, \quad \mathcal{P}_{i1} = \frac{1}{\sigma_{i1}} \frac{d\sigma_{i1}}{d\cos \theta}. \quad (3.31)$$

Then let us focus on the discrepancy between the entanglement entropies of final states for a given initial two-body state, $A_i B_i$ and $A_j B_j$:

$$\Delta S_{i,j} \equiv S_{i1} - S_{j1} = - \int_{-1}^1 d\cos \theta (\mathcal{P}_{i1} \ln \mathcal{P}_{i1} - \mathcal{P}_{j1} \ln \mathcal{P}_{j1}) \quad (i, j = 2, 3, \dots). \quad (3.32)$$

This quantity is independent of regularization, because V does not contribute to \mathcal{P}_{i1} and \mathcal{P}_{j1} .

Even though the regularization is necessary for the entanglement entropy of elastic channel, it is intriguing to consider the difference between the volume-regularized entanglement entropy of the elastic final state (3.29) and the one of the inelastic final state (3.30):

$$\Delta \tilde{S}_{2,1} \equiv \tilde{S}_{21} - \tilde{S}_{11} = - \int_{-1}^1 d\cos \theta (\mathcal{P}_{21} \ln \mathcal{P}_{21} - \tilde{\mathcal{P}}_{11} \ln \tilde{\mathcal{P}}_{11}). \quad (3.33)$$

Eq. (3.32) and Eq. (3.33) have formally same expression, which consists of cross sections and differential cross sections, in the form of the density distributions generated by $\tilde{\mathcal{P}}_{11}$ and \mathcal{P}_{21} .

4 Evaluation of entanglement entropy

4.1 Elastic and inelastic cross sections in the two-nucleon sector

We shall evaluate entanglement entropies in a high-energy proton-neutron scattering, as a prototype for the comparison of elastic and inelastic two-body cases. Their quantitative estimates can be performed using the neutron-proton scattering data. More precisely, the inelastic neutron-proton charge exchange reaction $pn \rightarrow np$ has been measured with a high-momentum neutron beam on a proton target [32]. The quantitative description of the elastic $pn \rightarrow pn$ cross sections can be obtained from the same two-body scattering with a forward neutron. One also may use data from the high-energy $pp \rightarrow pp$ scattering in the same energy range whose cross sections are equivalent, at least in the low momentum transfer range [33], as well as total cross sections. We thus are able to make use of the well documented phenomenology in that elastic case [34].

We thus focus on the following two-particle channels (see Fig. 1):

$$pn \rightarrow \begin{cases} pn & \text{(elastic channel)} \\ np & \text{(inelastic channel),} \end{cases} \quad (4.1)$$

where the first of the final particles is in the near forward (small t) range. We can recognize $pn \rightarrow np$ as an inelastic channel with charge one current exchange. In order to concretely

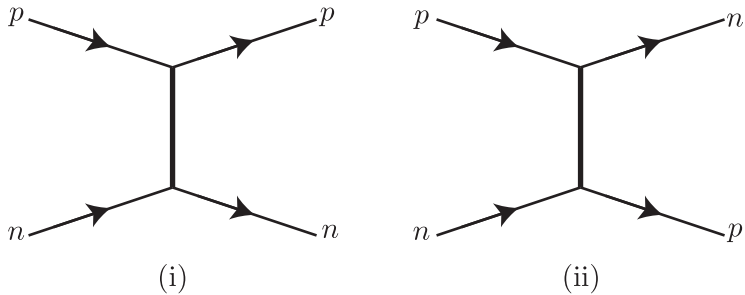


Fig. 1: (i) the elastic channel: $pn \rightarrow pn$. (ii) the inelastic channel: $pn \rightarrow np$.

evaluate the entanglement entropies, (3.29) and (3.30), the differential elastic and inelastic cross sections as functions of t and the total pn cross section are necessary.

For our analysis, we take advantage of obtaining the near forward proton-neutron elastic differential cross section from a precise phenomenological description of related amplitudes obtained from data on proton-proton elastic scattering, in Ref. [35] for differential cross sections in the forward region and in Refs. [36, 37] for total cross sections. The inelastic

differential cross section in the forward region is provided by Refs. [38, 39]. One finds the parameterizations of those observables used for our analysis in Appendix C.

4.2 Evaluation of the entanglement entropies in the two-nucleon sector

By using those fitting functions shown in the previous subsection, let us evaluate the elastic and inelastic entanglement entropies. Using the change of variable, $\cos \theta \rightarrow t$, by means of the relation (2.21), one writes the corresponding relation between density distributions,

$$\tilde{\mathcal{P}}(\cos \theta) d\cos \theta = P(t) dt. \quad (4.3)$$

One then infers from Eqs.(3.29) and (3.30), and the notations therein, that $P_{\text{el}}(t)$ (*resp.* $P_{\text{inel}}(t)$) defined by $P_{\text{el}}(t) = \frac{s-4m^2}{2} \tilde{\mathcal{P}}_{11}(\cos \theta)$ (*resp.* $P_{\text{inel}}(t) = \frac{s-4m^2}{2} \tilde{\mathcal{P}}_{21}(\cos \theta)$), where m is the nucleon mass, are the density distributions of the elastic (*resp.* inelastic) collisions in the transfer variable t . Naturally, $P_{\text{el,inel}}(t)$ satisfy $\int dt P_{\text{el,inel}}(t) = 1$.

We then rewrite the regularized entanglement entropies, (3.29) and (3.30), as

$$\tilde{S}_{\text{el}} = - \int_{-4k^2}^0 dt P_{\text{el}}(t) \ln \left(\frac{4\pi}{\sigma_{\text{tot}}} P_{\text{el}}(t) \right), \quad (4.4)$$

$$\tilde{S}_{\text{inel}} = - \int_{-4k^2}^0 dt P_{\text{inel}}(t) \ln \left(\frac{4\pi}{\sigma_{\text{tot}}} P_{\text{inel}}(t) \right). \quad (4.5)$$

It is important to note that the lower limit of integration in these equations is given by pure kinematics. But the physical limitation to the parameterizations for both elastic and inelastic cases are concentrated in their respective forward region, *i.e.* at small momentum transfer region. For instance, in the pn sector, $P_{\text{el}}(t)$ and $P_{\text{inel}}(t)$ are governed by very different parametric functions decreasing fastly with momentum transfer.

We numerically compute the elastic entanglement entropy (4.4) in terms of (C.1), (C.3) and (C.4). \tilde{S}_{el} has a local minimum at $\sqrt{s} = 41.7$ GeV. We then compute the inelastic entanglement entropy (4.5) in terms of (C.1), (C.5) and (C.16). \tilde{S}_{inel} has a local minimum at $\sqrt{s} = 12.4$ GeV. Both entropies are depicted in Fig. 2 as functions of the center-of-mass energy \sqrt{s} . The inelastic entanglement entropy is larger than the elastic one as shown in Fig. 2.

We also show in Fig. 3 the discrepancy (3.33) and the asymmetry between these two entropies, namely,

$$\Delta \tilde{S} = \tilde{S}_{\text{inel}} - \tilde{S}_{\text{el}}, \quad \text{asym } \tilde{S} = \frac{\tilde{S}_{\text{inel}} - \tilde{S}_{\text{el}}}{\tilde{S}_{\text{el}}}. \quad (4.6)$$

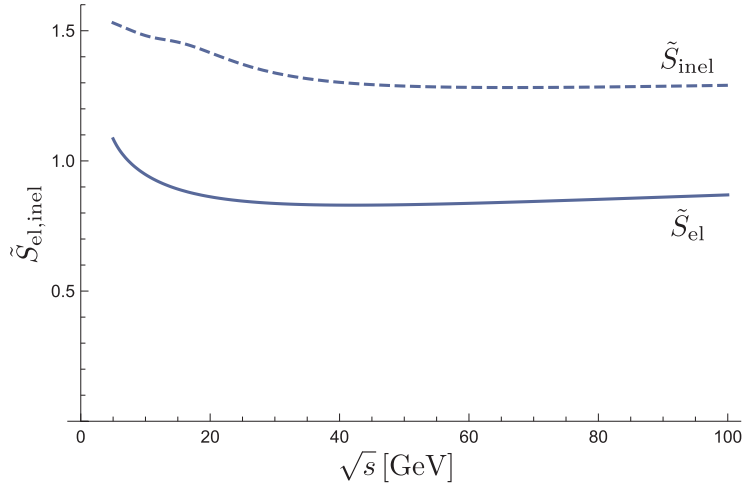


Fig. 2: The elastic entanglement entropy \tilde{S}_{el} (solid line) and the inelastic one \tilde{S}_{inel} (dashed line).

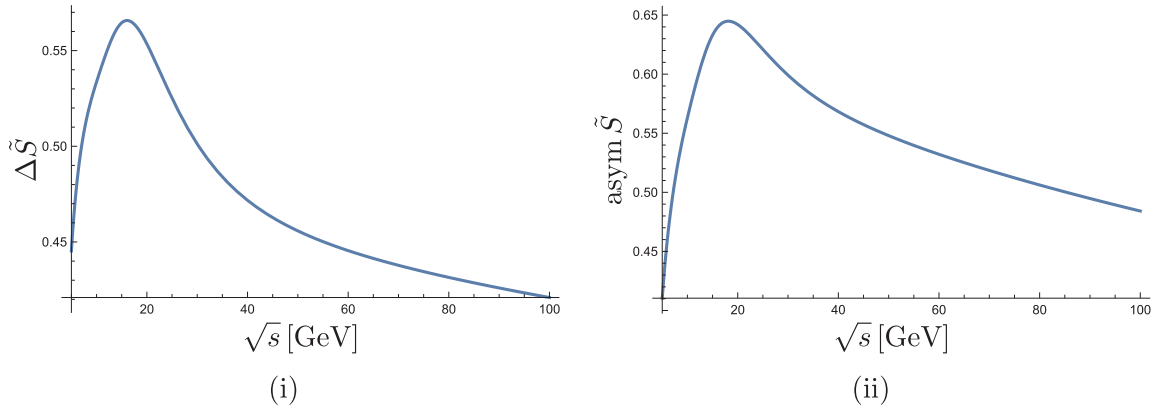


Fig. 3: (i) The difference $\Delta \tilde{S}$ and (ii) the asymmetry $\text{asym } \tilde{S}$ of entanglement entropies between the elastic and inelastic channels.

One can observe that at lower energy the elastic entanglement entropy decreases faster than the inelastic one while it is the contrary at higher energy as shown in Fig. 3.

The difference observed between the elastic and inelastic entanglement entropies for identical initial nucleons can be qualitatively interpreted using a simple exponential approximation of the dominant cross sections, following the treatment in Refs. [2, 3]. Let us write

$$\frac{d\sigma_{el}}{dt} \sim \sigma_{el}(s) e^{R_{el}^2 t}, \quad \frac{d\sigma_{inel}}{dt} \sim \sigma_{inel}(s) e^{R_{inel}^2 t}. \quad (4.7)$$

R_{el} and R_{inel} are the effective radii. Using formulas (4.4) and (4.5), one easily finds

$$\tilde{S}_{\text{el}} = \ln \left(\frac{\sigma_{\text{tot}}}{4\pi R_{\text{el}}^2} \right) + 1, \quad (4.8)$$

$$\tilde{S}_{\text{inel}} = \ln \left(\frac{\sigma_{\text{tot}}}{4\pi R_{\text{inel}}^2} \right) + 1, \quad (4.9)$$

$$\Delta \tilde{S} = \tilde{S}_{\text{inel}} - \tilde{S}_{\text{el}} = \ln \left(\frac{R_{\text{el}}^2}{R_{\text{inel}}^2} \right). \quad (4.10)$$

Hence, the inelastic scattering being smoother in momentum transfer than the elastic one at comparable energies, see Refs. [32, 34], one has $R_{\text{inel}}^2 < R_{\text{el}}^2$ and thus $S_{\text{inel}} > S_{\text{el}}$, as quantitatively confirmed by the full calculations, see Fig. 2. Smaller is the effective radius, larger is the entanglement between the final couple of particles.

4.3 Density of entanglement entropy in transverse momentum

The integral equations for entanglement entropies (4.4) and (4.5) can be rewritten

$$\tilde{S}_{\text{el}} = \int_0^{4k^2} d|t| D_{\text{el}}(t), \quad D_{\text{el}}(t) \equiv -P_{\text{el}}(t) \ln \left(\frac{4\pi}{\sigma_{\text{tot}}} P_{\text{el}}(t) \right), \quad (4.11)$$

$$\tilde{S}_{\text{inel}} = \int_0^{4k^2} d|t| D_{\text{inel}}(t), \quad D_{\text{inel}}(t) \equiv -P_{\text{inel}}(t) \ln \left(\frac{4\pi}{\sigma_{\text{tot}}} P_{\text{inel}}(t) \right). \quad (4.12)$$

Note again, as for Eqs. (4.4) and (4.5), the upper bound of integration is given by kinematics, but the physical focus (together with the parameterizations) is on the different forward regions of the two reactions.

Thus we obtain the expressions for the entropy densities, D_{el} and D_{inel} , as functions of the transfer momentum $q_T = \sqrt{|t|}$. Note that $D_{\text{el,inel}}$ as well as $P_{\text{el,inel}}$ are also functions of the energy variable which is implicit.

Indeed, the physical interpretation of these densities are interesting: they describe the local amount of entanglement entropy flow as a function of momentum transfer for a given total energy \sqrt{s} . As depicted in Fig. 4, the elastic entropy flow D_{el} and the inelastic one D_{inel} at $\sqrt{s} = 20$ GeV are both stronger and similar in the very forward direction. They both decrease when the momentum transfer increases but the inelastic one then dominates by orders of magnitude. This is the cause of the different trend revealed in Fig. 2 for the overall entanglement entropies.

One thus understands that entanglement is stronger when the particle trajectories are very near-by as expected but the exchange of a non-vacuum quantum number, namely the

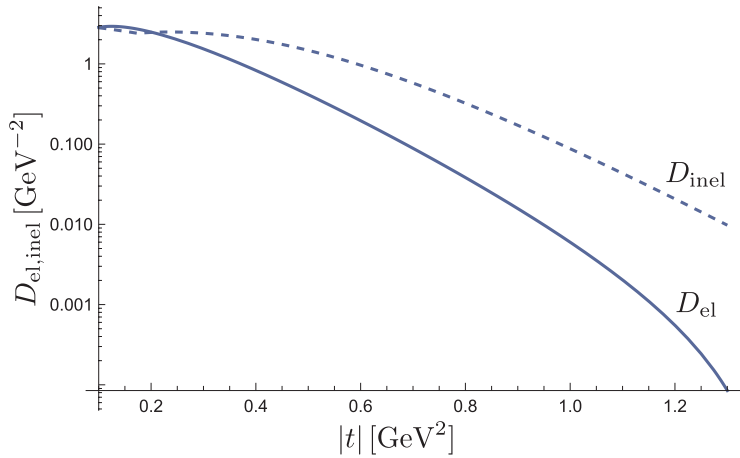


Fig. 4: The elastic density D_{el} (solid line) and the inelastic one D_{inel} (dashed line) as functions of $|t|$ at $\sqrt{s} = 20$ GeV

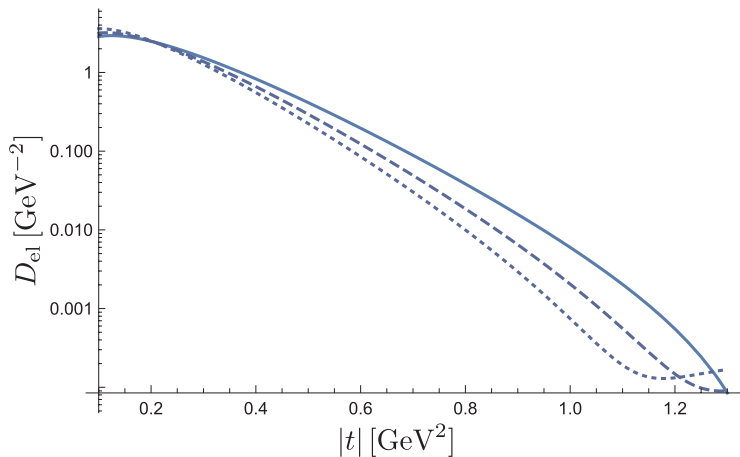


Fig. 5: The elastic density D_{el} as a function of $|t|$ at $\sqrt{s} = 20$ GeV (solid line), 50 GeV (dashed line) and 100 GeV (dotted line).

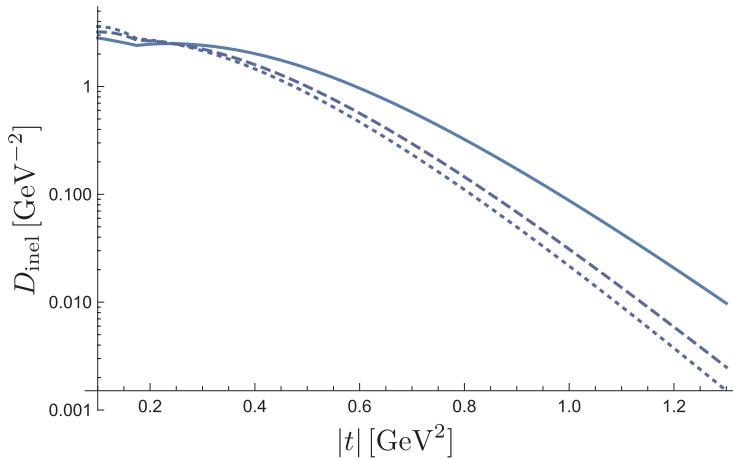


Fig. 6: The inelastic density D_{inel} as a function of $|t|$ at $\sqrt{s} = 20$ GeV (solid line), 50 GeV (dashed line) and 100 GeV (dotted line).

electric charge in our case, seems to keep on longer distances the entanglement between the final particles. This property obtained in the two nucleon sector would be interesting to be investigated elsewhere.

Interestingly, the quasi equality between both densities in the very forward region seen in Fig. 4 seems to indicate that the selection process for a proton or a neutron in the very forward scattering, which has a strong consequence for the hierarchy of the energy dependence of the differential cross sections, does not modify the entanglement in this very forward region. By contrast, both for the elastic or the inelastic scattering considered as a function of their own energy dependence, there is a similar trend of the densities as shown by Figs. 5 and 6 despite the very different energy dependence of the differential cross sections.

5 Conclusion and outlook

Let us summarize our results.

We have performed the formalism allowing to derive the entanglement entropies in parallel for elastic and inelastic two-body reactions at high energy. Once using the “volume” regularization characterized by the total cross sections of the incident particles, the elastic and inelastic entanglement entropies have a similar expression, and enable us to study various relations between the entanglement entropy for different final two-body state channels.

As a typical application of the formalism and an example of the mentioned relations, we have evaluated the entanglement entropy in the two-nucleon sector, namely, $pn \rightarrow pn$, in the forward region for the elastic scattering, and $pn \rightarrow np$ in the forward region for the inelastic

scattering.

Remarkably, using parameterizations of data in the same energy range at $\sqrt{s} = 20, 50$ and 100 GeV for both elastic and inelastic pn scatterings, we find a marked difference between their entanglement entropies, the inelastic entanglement entropy being significantly stronger than the elastic one. By contrast, the energy dependence in both channels is rather mild, with a slight increase at higher energies. This is contrasted with the cross-section dependence which are polynomially decreasing for the inelastic channels contrary to the elastic one.

As an interesting output of our formulation, we obtain the density of entanglement entropy as a function of transverse momentum squared $q_T^2 = |t|$, which allows for a detailed description of the entropy flow in the various reactions. Applied to the two-nucleon sector, we find that both densities of the elastic and inelastic cases are equal in the very forward region $|t|$, while the inelastic density more and more dominates the elastic one, explaining the difference in the overall entropy.

In outlook, we would like to emphasize some interesting further studies allowed by our formalism. At first, it will be interesting to evaluate the elastic-inelastic channel relation for all cases where data exist. This would help answering quite fundamental questions:

- Is there a common feature that vacuum quantum number exchange (elastic case) would generate less entanglement than non-vacuum exchange (inelastic case)?
- The study of the entanglement entropy density as a function of transverse momentum seems to open a window on the flow of entanglement in a two-body scattering. Is there some regularity of this flow for different initial particles indicating some universality properties?

All in all, the goal is to understand the key features of entanglement in momentum due to the interaction and understand which are the order parameters to which it obeys: initial particle quantum numbers, exchange quantum numbers, eventually some particular energy ranges, *etc..*

Acknowledgments

S. S. was supported in part by JSPS Grant-in-Aid for Scientific Research (C) #22K03625, and is grateful to Institut de Physique Théorique (IPhT), CEA-Saclay for their hospitality.

A Dirac delta function and Legendre polynomials

The three-dimensional Dirac delta function in spherical coordinates with azimuthal symmetry can be written as

$$\delta^{(3)}(\mathbf{p} - \mathbf{k}) = \frac{\delta(p - k)}{4\pi k^2} \sum_{\ell=0}^{\infty} (2\ell + 1) P_{\ell}(\cos \theta), \quad (\text{A.1})$$

with $\cos \theta = (\mathbf{p} \cdot \mathbf{k})/(pk)$. Taking the limit $\mathbf{p} \rightarrow \mathbf{k}$, we obtain

$$\frac{4\pi k^2 \delta^{(3)}(0)}{\delta(0)} = \sum_{\ell=0}^{\infty} (2\ell + 1) P_{\ell}(1) = \sum_{\ell=0}^{\infty} (2\ell + 1). \quad (\text{A.2})$$

B Dirac delta function for energy conservation

We fix the center-of-mass energy of two incoming particles as

$$\sqrt{s} = E_{A_j \mathbf{k}} + E_{B_j \mathbf{k}} = \sqrt{m_{A_j}^2 + k^2} + \sqrt{m_{B_j}^2 + k^2} \quad (\text{B.1})$$

Then we compute the delta function for energy conservation,

$$\begin{aligned} \delta((E_{A_h \mathbf{q}} + E_{B_h \mathbf{q}}) - (E_{A_j \mathbf{k}} + E_{B_j \mathbf{k}})) &= \delta((E_{A_h \mathbf{q}} + E_{B_h \mathbf{q}}) - \sqrt{s}) \\ &= \delta\left(\frac{q\sqrt{s}}{E_{A_h \mathbf{q}} E_{B_h \mathbf{q}}}(q - q') + \mathcal{O}((q - q')^2)\right) \\ &= \frac{2E_{A_h \mathbf{q}} 2E_{B_h \mathbf{q}}}{4q\sqrt{s}} \delta(q - q'). \end{aligned} \quad (\text{B.2})$$

q' is given by $(E_{A_h \mathbf{q}'} + E_{B_h \mathbf{q}'}) - \sqrt{s} = 0$, that is,

$$q' = \sqrt{\frac{(m_{A_h}^2 + m_{B_h}^2 - s)^2 - 4m_{A_h}^2 m_{B_h}^2}{4s}}. \quad (\text{B.3})$$

C Parameterizations of the elastic and inelastic pn cross sections.

C.1 Total cross section

The same pn total cross section appears in both the elastic and inelastic entanglement entropies, (3.29) and (3.30). We can read it from the parameterization of the total pp cross sections, arguing from the equivalence with pn forward scattering. From Refs. [36, 37], one reads

$$\sigma_{\text{tot}} = -\frac{1}{s} \text{Im}(M_+(s) - M_-(s)) [\text{GeV}^{-2}], \quad (\text{C.1})$$

with

$$\text{Im } M_+(s) = -s(163 - 20.4 \ln s + 1.75(\ln s)^2), \quad \text{Im } M_-(s) = -73.1s^{0.48}. \quad (\text{C.2})$$

By definition in [36, 37], M_\pm imply amplitudes such that $M_\pm = \frac{1}{2}(M_{pp} \pm M_{p\bar{p}})$.

C.2 Elastic cross sections

In Ref. [35] one can read the elastic pp differential cross section (equivalent to $pn \rightarrow pn$ ones in the forward region);

$$\frac{d\sigma_{\text{el}}}{dt} = \left| i 6.88 e^{(2.69+0.306 \ln s - i 0.153\pi)t} + \left(\frac{10.3}{s} - i 0.035 \right) e^{0.89t} \right|^2 [\text{mb} \cdot \text{GeV}^{-2}]. \quad (\text{C.3})$$

Then the elastic cross section is given, neglecting the exponentially small tail at large transfer, by

$$\sigma_{\text{el}} = \int_{-\infty}^0 dt \frac{d\sigma_{\text{el}}}{dt} \quad (\text{C.4})$$

C.3 Inelastic cross sections

Refs. [38, 39] have shown three models of the inelastic differential cross section for $pn \rightarrow np$ with similar overall results. We adopt the two-component model [38] using the first component defined in [39].

The inelastic differential cross section based on the 5-helicity amplitudes,

$$\frac{d\sigma_{\text{inel}}}{dt} = \frac{2\pi}{s^2} 0.389 (|\varphi_1|^2 + |\varphi_2|^2 + |\varphi_3|^2 + |\varphi_4|^2 + |\varphi_5|^2). \quad (\text{C.5})$$

φ_i is split into an energy-independent part φ_i^c and an energy-dependent part φ_i^v , *i.e.*, $\varphi_i = \varphi_i^c + \varphi_i^v$. From Refs. [38, 39] we write down φ_i^c ,

$$\varphi_1^c = 15 \frac{t}{s-4m^2} \frac{m^2}{s} (-2.2) e^{5t}, \quad (\text{C.6})$$

$$\varphi_2^c = 15 \left\{ \frac{t}{t-m_\pi^2} + \frac{4t}{m^2} - 0.9 - \frac{0.45t}{s-4m^2} + \frac{0.65t}{s-4m^2} \frac{m^2}{s} + \frac{0.65t}{s-4m^2} \left(\frac{m^2}{s} + 0.5 \right) \right\} e^{5t}, \quad (\text{C.7})$$

$$\varphi_3^c = 0, \quad (\text{C.8})$$

$$\varphi_4^c = 15 \left\{ \frac{t}{t-m_\pi^2} + \frac{4t}{m^2} + \frac{t}{s-4m^2} \left(1.55 \frac{m^2}{s} + 0.325 \right) \right\} e^{5t}, \quad (\text{C.9})$$

$$\varphi_5^c = 15 \frac{m^2}{s-4m^2} \sqrt{-\frac{t}{4m^2} \frac{s-4m^2+t}{s}} 2.2 e^{5t}, \quad (\text{C.10})$$

where the nucleon mass, $m = 0.939 \text{ GeV}$, and the pion mass, $m_\pi = 0.139 \text{ GeV}$. One can reads φ_i^v from Eqs. (2a,b,c) and Eqs. (4b,c) in [38] as follows:

$$\varphi_1^v = \varphi_3^v = \beta_{\text{eff}}(t) s^{\alpha_{\text{eff}}(t)}, \quad (\text{C.11})$$

$$\varphi_2^v = -\varphi_4^v = 17t \beta_{\text{eff}}(t) s^{\alpha_{\text{eff}}(t)}, \quad (\text{C.12})$$

$$\varphi_5^v = -\sqrt{-17t} \beta_{\text{eff}}(t) s^{\alpha_{\text{eff}}(t)}, \quad (\text{C.13})$$

where

$$\alpha_{\text{eff}}(t) = \begin{cases} 0.74 + 0.67t & (|t| < 0.175) \\ 0.63 + 0.04t & (|t| > 0.175) \end{cases} \quad (\text{C.14})$$

$$\beta_{\text{eff}} = -0.12e^{5.5t}. \quad (\text{C.15})$$

Then the inelastic cross section is calculated through

$$\sigma_{\text{inel}} = \int_{-\infty}^0 dt \frac{d\sigma_{\text{inel}}}{dt}. \quad (\text{C.16})$$

C.4 Uncertainties

The error bars obtained for the total pn cross-sections and for the differential elastic ones are negligible, thanks to the use of the equivalent pp total [36,37] and differential [35] cross-sections whose data and their phenomenological description are well documented.

For the inelastic $pn \rightarrow np$ cross sections the two-component model we considered leads to a $\chi^2/6 \leq 1$ for six energies and for each of 24 among 28 data points in $|t|$ [38]. This is quite satisfactory taking into account that experimental results are less precise due to the necessary use of neutron incident particles.

References

- [1] V. Balasubramanian, M. B. McDermott and M. Van Raamsdonk, “Momentum-space entanglement and renormalization in quantum field theory,” Phys. Rev. D **86** (2012), 045014 [arXiv:1108.3568 [hep-th]].
- [2] R. Peschanski and S. Seki, “Entanglement Entropy of Scattering Particles,” Phys. Lett. B **758** (2016) 89 [arXiv:1602.00720 [hep-th]].

- [3] R. Peschanski and S. Seki, “Evaluation of Entanglement Entropy in High Energy Elastic Scattering,” *Phys. Rev. D* **100** (2019) no.7, 076012 [arXiv:1906.09696 [hep-th]].
- [4] T. N. Tomaras and N. Toumbas, “IR dynamics and entanglement entropy,” *Phys. Rev. D* **101** (2020) no.6, 065006 [arXiv:1910.07847 [hep-th]].
- [5] M. Rigobello, S. Notarnicola, G. Magnifico and S. Montangero, “Entanglement generation in (1+1)D QED scattering processes,” *Phys. Rev. D* **104** (2021) no.11, 114501 [arXiv:2105.03445 [hep-lat]].
- [6] J. Fan, G. M. Deng and X. J. Ren, “Entanglement entropy and monotones in scattering process,” *Phys. Rev. D* **104** (2021) no.11, 116021 [arXiv:2112.04254 [hep-th]].
- [7] J. D. Fonseca, B. Hiller, J. B. Araujo, I. G. da Paz and M. Sampaio, “Entanglement and scattering in quantum electrodynamics: S matrix information from an entangled spectator particle,” *Phys. Rev. D* **106** (2022) no.5, 056015 [arXiv:2112.01300 [quant-ph]].
- [8] S. Fedida and A. Serafini, “Tree-level entanglement in quantum electrodynamics,” *Phys. Rev. D* **107** (2023) no.11, 116007 [arXiv:2209.01405 [quant-ph]].
- [9] S. Fedida, A. Mazumdar, S. Bose and A. Serafini, “Entanglement entropy in scalar quantum electrodynamics,” *Phys. Rev. D* **109** (2024) no.6, 065028 [arXiv:2401.10332 [hep-th]].
- [10] M. Blasone, S. De Siena, G. Lambiase, C. Matrella and B. Micciola, “Complete complementarity relations in tree level QED processes,” *Phys. Rev. D* **111** (2025) no.1, 016007 [arXiv:2402.09195 [quant-ph]].
- [11] Q. Liu, I. Low and Z. Yin, “Quantum Magic in Quantum Electrodynamics,” [arXiv:2503.03098 [quant-ph]].
- [12] M. Blasone, S. De Siena, G. Lambiase, C. Matrella and B. Micciola, “Entanglement dynamics in QED processes,” *Chaos Solitons Fractals* **195** (2025), 116305.
- [13] J. Fan, Y. Deng and Y. C. Huang, “Variation of entanglement entropy and mutual information in fermion-fermion scattering,” *Phys. Rev. D* **95** (2017) no.6, 065017 [arXiv:1703.07911 [hep-th]].

- [14] J. Fan and X. Li, “Relativistic effect of entanglement in fermion-fermion scattering,” *Phys. Rev. D* **97** (2018) no.1, 016011 [arXiv:1712.06237 [hep-th]].
- [15] D. E. Kharzeev and E. M. Levin, “Deep inelastic scattering as a probe of entanglement,” *Phys. Rev. D* **95** (2017) no.11, 114008 [arXiv:1702.03489 [hep-ph]].
- [16] G. S. Ramos and M. V. T. Machado, “Investigating entanglement entropy at small- x in DIS off protons and nuclei,” *Phys. Rev. D* **101** (2020) no.7, 074040 [arXiv:2003.05008 [hep-ph]].
- [17] E. Levin, “Multiplicity distribution and entropy of produced gluons in deep inelastic scattering at high energies,” *Eur. Phys. J. C* **84** (2024) no.7, 662 [arXiv:2306.12055 [hep-ph]].
- [18] G. Grignani and G. W. Semenoff, “Scattering and momentum space entanglement,” *Phys. Lett. B* **772** (2017), 699-702 [arXiv:1612.08858 [hep-th]].
- [19] A. Bose, P. Haldar, A. Sinha, P. Sinha and S. S. Tiwari, “Relative entropy in scattering and the S-matrix bootstrap,” *SciPost Phys.* **9** (2020), 081 [arXiv:2006.12213 [hep-th]].
- [20] G. S. Ramos and M. V. T. Machado, “Determination of entanglement entropy in elastic scattering using the model-independent method for hadron femtoscopy,” *Phys. Rev. D* **102** (2020) no.3, 034019 [arXiv:2007.09744 [hep-ph]].
- [21] G. A. Miller, “Entanglement of elastic and inelastic scattering,” *Phys. Rev. C* **108** (2023) no.4, L041601 [arXiv:2306.14800 [nucl-th]].
- [22] U. Gürsoy, D. E. Kharzeev and J. F. Pedraza, “Universal rapidity scaling of entanglement entropy inside hadrons from conformal invariance,” *Phys. Rev. D* **110** (2024) no.7, 074008 [arXiv:2306.16145 [hep-th]].
- [23] M. Blasone, G. Lambiase and B. Micciola, “Entanglement distribution in Bhabha scattering with an entangled spectator particle,” *Phys. Rev. D* **109** (2024) no.9, 096022 [arXiv:2401.10715 [quant-ph]].
- [24] R. Aoude, G. Elor, G. N. Remmen and O. Sumensari, “Positivity in Amplitudes from Quantum Entanglement,” [arXiv:2402.16956 [hep-th]].
- [25] K. Kowalska and E. M. Sessolo, “Entanglement in flavored scalar scattering,” *JHEP* **07** (2024), 156 [arXiv:2404.13743 [hep-ph]].

[26] I. Low and Z. Yin, “Elastic cross section is entanglement entropy,” Phys. Rev. D **111** (2025) no.6, 065027 [arXiv:2410.22414 [hep-th]].

[27] J. Thaler and S. Trifinopoulos, “Flavor patterns of fundamental particles from quantum entanglement?,” Phys. Rev. D **111** (2025) no.5, 056021 [arXiv:2410.23343 [hep-ph]].

[28] J. Liu, M. Tanaka, X. P. Wang, J. J. Zhang and Z. Zheng, “Scattering entanglement entropy and its implications for electroweak phase transitions,” Phys. Rev. D **112** (2025) no.1, 015028 [arXiv:2505.06001 [hep-ph]].

[29] C. M. Sou, Y. Wang and X. Zhang, “Entanglement features from heavy particle scattering,” [arXiv:2507.03555 [hep-th]].

[30] L. Van Hove, “A Phenomenological Discussion of Inelastic Collisions at High Energies,” Nuovo Cim. **28** (1963) 2344.

[31] A. Białas and L. Van Hove, “Two-Particle and Many-Particle Channels in High-Energy Collisions,” Nuovo Cim. **38** (1965) 1385.

[32] M. N. Kreisler, M. B. Davis, M. J. Longo and D. D. O’Brien, “Neutron-Proton Charge Exchange Scattering from 8-GeV/c to 29-GeV/c,” Nucl. Phys. B **84** (1975), 3.

[33] C. E. Dehaven, C. A. Ayre, H. R. Gustafson, L. W. Jones, M. J. Longo, P. V. Ramana Murthy, T. J. Roberts and M. R. Whalley, “Neutron-proton differential cross sections in the range 70 to 400 GeV/ c,” Nucl. Phys. B **148** (1979), 1-17.

[34] N. Kwak, E. Lohrmann, E. Nagy, M. Regler, W. Schmidt-Parzefall, K. R. Schubert, K. Winter, A. Brandt, H. Dibon and G. Flugge, *et al.* “Experimental Results on Large Angle Elastic $p\bar{p}$ Scattering at the CERN ISR,” Phys. Lett. B **58** (1975), 233.

[35] R. J. N. Phillips and V. D. Barger, “Model independent analysis of the structure in $p\bar{p}$ scattering,” Phys. Lett. B **46** (1973), 412.

[36] M.M. Block and R. Cahn, “Forward hadronic $p\bar{p}$ and $\bar{p}p$ elastic scattering amplitudes: Analysis of existing data and extrapolations to collider energies,” Phys. Lett. B **120B** (1983) 224.

[37] M.M. Block and R. Cahn, “Near Forward $p\bar{p}$ and $\bar{p}p$ Elastic Scattering: Slope Analysis of Existing Data,” Phys. Lett. B **120B** (1983) 229.

- [38] A. Bouquet and B. Diu, “The Energy Dependence of Neutron-Proton Charge Exchange,” *Nuovo Cim. A* **43** (1978), 53.
- [39] G. Bizard and B. Diu, “Phenomenological FIT of the n p Charge-Exchange Cross-Section at Intermediate and High-Energy,” *Nuovo Cim. A* **25** (1975), 467.